LETTER

Correspondence between the Hamiltonian cycle problem and the quantum $\mathbb{Z}_2$ lattice gauge theory

To cite this article: Xiaopeng Cui and Yu Shi 2023 *EPL* **144** 48001

A Letters Journal Exploring the Frontiers of Physics

November 2023

EPL, **144** (2023) 48001
doi: 10.1209/0295-5075/ad130b

www.epljournal.org

Correspondence between the Hamiltonian cycle problem and the quantum $\mathbb{Z}_2$ lattice gauge theory

Xiaopeng Cui and Yu Shi[(a)]

Shanghai Research Center for Quantum Science and CAS Center for Excellence in Quantum Information and Quantum Physics, University of Science and Technology of China - Shanghai 201315, China, University of Science and Technology of China - Hefei 230026, China and Department of Physics & State Key Laboratory of Surface Physics, Fudan University - Shanghai 200433, China

received 20 October 2023; accepted in final form 6 December 2023
published online 21 December 2023

Abstract – We propose the correspondence between the Hamiltonian cycle (HC) problem in graph theory and the quantum $\mathbb{Z}_2$ lattice gauge theory (QZ2LGT) defined on the lattice dual to that graph. For the QZ2LGT, when the coupling parameter g is less than the critical value g_c, the ground state is a superposition of all configurations with closed strings of same spins, which can be obtained by using an adiabatic quantum algorithm. A subsequent search for a HC among those closed strings solves the original HC problem. The method is demonstrated for random samples of small graphs.

Introduction. – A well-known problem in graph theory is the HC problem [1]. On an undirected graph, made up of a number of vertices connected by a number of edges without directions [2], a HC is a cycle that visits each vertex exactly once. The HC problem is to determine whether such a HC exists. The HC problem is a NP complete problem. Gauge theory is the framework describing the fundamental interactions in particle physics, as well as strong correlations in condensed matter physics. Lattice gauge theory (LGT) is an approach to gauge theories by discretizing the spacetime or space to a lattice. QZ2LGT is the simplest LGT [3,4]. Recently quantum simulation has become a new approach to LGT, including QZ2LGT [5–8]. Meanwhile, various kinds of progress are made in interplay between quantum information science and graph theory, for example, entanglement in multi-qubit graph states [9], chip-based photonic graph states [10], and coherent Ising machine [11].

In this paper, we propose the correspondence between the HC problem and QZ2LGT. We regard a graph as the dual of a lattice, on which the QZ2LGT is defined. Thus each vertex of the graph maps to a plaquette in the lattice, each edge in the graph crosses a link in the dual lattice, and two adjacent vertices in the graph correspond to two adjacent plaquettes in the lattice. The length is not defined for each edge in the graph or each link in the lattice, therefore the lattice can be deformed.

[(a)]E-mail: yushi@fudan.edu.cn (corresponding author)

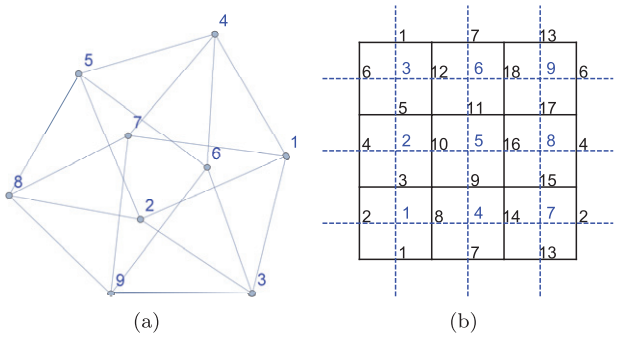

Fig. 1: Correspondence between a graph and its dual. (a) A graph corresponding to the 3×3 lattice shown in (b). (b) 3×3 toroid lattice, where the black solid lines are links, the blue dotted lines correspond to the edges of the graph in (a), the numbers in black denote the edges of the lattice, and the numbers in blue correspond to those for the vertices in the graph in (a).

Thus an undirected unweighted graph of N_v vertices becomes the dual of a lattice with N_v palquettes. Depicted in fig. 1 is an example in which the graph becomes the dual of a 3×3 square lattice, with periodic boundary condition, *i.e.*, a topologically toroid lattice.

In this way, a HC in a graph is just a HC in the dual of a lattice. By connecting the last with the first visited vertices in the original graph, an HC in the original graph becomes a closed string or loop passing through all the plaquettes of the lattice with periodic boundary condition,

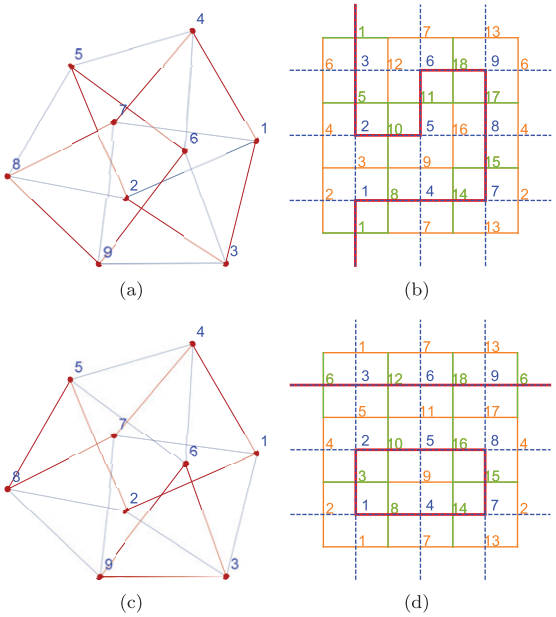

Fig. 2: Identification of the cycles on a certain graph as the closed strings on the dual of a square lattice. (a) A HC of the graph, depicted as a red path in (a) becomes a closed string passing through all the plaquettes on the dual, depicted in red in (b). (b) A configuration of closed strings at the ground state of QZ2LGT at $g = 0$. There is only one closed string, depicted as a red path. The orange edge is in $|0\rangle$, the green edge is in $|1\rangle$. (c) Two cycles in the graph, depicted in red. (d) A closed string configuration in QZ2LGT ground state at $g = 0$, with two closed strings, depicted as red paths, corresponding to the two cycles in the graph. The orange edge is in $|0\rangle$, and the green edge is in $|1\rangle$.

as shown in fig. 2(a), (b) and fig. 2(c), (d). Hence the HC problem becomes the search for a closed string that visits each vertex of the dual lattice once. This is much easier, since the set of all the closed strings is much smaller than the set of all paths.

Furthermore, the search for a HC among the closed strings can be significantly facilitated by the topological quantum phase transition (TQPT) in QZ2LGT. A TQPT occurs at the critical value g_c of the coupling parameter g, separating the confined phase for $g > g_c$ and the deconfined phase for $g < g_c$, at which the ground state is a quantum superposition of all configurations of closed strings of down spins, called closed-string condensation [12,13]. g_c depends on the properties of the graph, including the number of HCs, denoted as N_{hc}. Therefore, reaching TQPT in a quantum adiabatic simulation becomes the key step in the present approach to the HC problem. This method applies to any graph, which can always be regarded as dual to a lattice on which QZ2LGT can always be defined.

Quantum $\mathbb{Z}_2$ LGT and closed strings. – The Hamiltonian of QZ2LGT is [4,7,14]

$$H = Z + gX, \tag{1}$$

with $X = -\sum_l \sigma_l^x$, $Z = \sum_\square Z_\square$, $Z_\square = -\prod_{l\in\square} \sigma_l^z$, where the spins (qubits) occupy the links l's, $\square$ represents the elementary plaquette of the lattice. Single-spin states $|0\rangle$ and $|1\rangle$ correspond to $\sigma_l^z = 1$ (up) and $\sigma_l^z = -1$ (down), respectively. The ground state at $g = 0$ is

$$|\psi_0\rangle = \sum_{i=1}^{S_0} |\phi_i\rangle, \tag{2}$$

where each $|\phi_i\rangle$ is with $Z_\square = -1$ for any $\square$. In the $M \times N$ torus lattice, there are $N_v \equiv MN$ vertices, $N_e \equiv 2N_v$ links, and the number of plaquettes N_p equals N_v. Hence the number of configurations with $Z_\square = -1$ for any $\square$ is $S_0 \equiv 2^{N_e}/(2^{N_v-1})$, where 2^{N_e} is the number of all possible configurations of spins, as each edge is occupied by one spin, while $1/2^{N_v-1}$ is the probability that $Z_\square = -1$ for each $\square$.

On the lattice on which QZ2LGT is defined, one can regard a link with spin $\sigma_l^z = -1$ as occupied, while a link with spin $\sigma_l^z = 1$ as unoccupied. Occupied links can be connected to form a string, which may be open or closed, then $|\phi_i\rangle$ can be regarded as a configuration of closed strings of down spins. When $g < g_c$, the ground state can be represented as a closed-string condensate, which is a superposition of S_0 configurations of closed strings. Especially, when $g = 0$, the superposition is of equal amplitude [12,15,16]. Among the S_0 configurations of closed strings, one example is shown in fig. 2(a), (b), where a single closed string passes through all N_v plaquettes of the lattice, and is thus a HC. Another example is shown in fig. 2(c), (d), where there are two closed strings, each passing through a part of the N_v plaquettes, so there is no HC.

Therefore, in order to solve the HC problem, one only needs to search for HCs in the S_0 configurations of closed strings, rather than $N_v!$ configurations in the original configuration space [2]. This greatly reduces complexity.

Quantum adiabatic algorithm. – Now we present the quantum adiabatic algorithm of HCP, by mapping it to a search for closed strings in the ground state of QZ2LGT. It consists of two consecutive processes. The first is to obtain the closed-string condensate, the second is to search for closed strings in it.

In the adiabatic process, the initial state is the ground state at $g = +\infty$, which is the equal superposition of all product states of $|0\rangle$ and $|1\rangle$. With g decreased adiabatically towards $g \leq g_c$, the closed-string condensate is obtained. This process is equivalent to adiabatically evolve $H_\lambda = \lambda Z + X$, with $\lambda = \frac{1}{g}$, from $\lambda = 0$ towards $\lambda_c = \frac{1}{g_c}$. To satisfy the adiabatic condition, the time scale is $t = O(\sqrt{N_e})$ for a 2-dimensional lattice [17]. Hence for a lattice with unknown λ_c, in the adiabatic algorithm, in which λ uniformly increases from 0, the time scale is $t = O(\sqrt{N_e})\lambda_c$.

For the adiabatic evolution, we decompose the unitary evolution by using the symmetric Trotter

decomposition, which is more efficient than the original Trotter decomposition [18,19]. The error for each step in the adiabatic simulation is $\varepsilon_s(t,n,g) = |e^{-i(A+B)t} - (e^{-iA\frac{t}{2n}}e^{-iB\frac{t}{n}}e^{-iA\frac{t}{2n}})^n| = |e^{-i(A+B)t} - e^{-iA\frac{t}{2n}}(e^{-iB\frac{t}{n}}e^{-iA\frac{t}{n}})^{n-1}e^{-iB\frac{t}{n}}e^{-iA\frac{t}{2n}}| \leqslant (\frac{1}{12}g^2N_vn_l^2 + \frac{1}{24}gN_e * n_p^2)\frac{t^3}{n^2}$, where $A = Z$ and $B = gX$ are the two terms in the Hamiltonian, t is the time of the step, n is the number of symmetric Trotter substeps, n_l is the number of links surrounding each plaquette, n_p is the number of vertices connected by each edge or is the number of plaquettes sharing each link [7]. Then the cumulative error from the start to the phase transition point λ_c can be obtained as $\varepsilon = O(\frac{1}{N_{ss}^2}N_e^{3/2}(N_v^3 + N_e\lambda_c)\lambda_c^4)$, where N_{ss} is the total number of symmetric Trotter substeps. Therefore, the time complexity required in the adiabatic quantum simulation QZ2LGT is $O_1 = O(\sqrt{\frac{1}{\varepsilon}N_e^{3/2}(N_v^3 + N_e\lambda_c)\lambda_c^4}) = O(\frac{1}{g_c^2}\sqrt{\frac{1}{\varepsilon}N_e^{3/2}(N_v^3 + \frac{N_e}{g_c})})$, where ε is reinterpreted as the precision required for the quantum simulation. In a connected undirected graph, $N_v \leq N_e \leq N_v(N_v-1)/2$, g_c, λ_c are fixed quantities for a given graph.

Subsequently, a quantum search algorithm searches for HCs in the closed-string condensate, which is is a superposition of $S_0 = O(2^{N_e}/2^{N_v})$ components, including those with HCs. The time complexity is $O_2 \sim \frac{S_0}{N_{hc}}$, since the probability of obtaining a state with a HC in a measurement is $\frac{N_{hc}}{S_0}$. The relationship between N_{hc} and N_e of some sample graphs will be studied below. The time complexity for the whole process is $O = O_1O_2$.

After reaching the TQPT, a measurement of g_c contributes additional time complexity O_M. According to the phase estimation method [7], O_M is of the same order of magnitude as O_1. Thus with adiabatic algorithm followed by measurement, we have a quantum algorithm for finding g_c, with time complexity $O' = O_1 + O_M \sim O_1$.

Relations between g_c and the graph properties. – The complexity O_1 depends on $\lambda_c \equiv \frac{1}{g_c}$. g_c depends on the properties of the graph, and thus may reveal latter, for example, N_{hc} and N_e. Hence we need to investigate the relations between g_c on one hand, and the graph properties such as N_{hc}, N_e and the degree of the vertices on the other.

We work on this problem using the classical demonstration of the quantum adiabatic simulation, in terms of the QuEST simulator [20]. The hardware we use is the Nvidia GPU Tesla V100-SXM2-32GB [7].

We first randomly generate four graphs with $N_v = 9$ and $N_e = 18$, as shown in fig. 3. The fourth corresponds to the 3×3 toroid lattice. N_{hc} of the four graphs are 0, 10, 30 and 48, respectively. For such small graphs, we use the so-called measurement method [7] to obtain the ground state $|\psi_0\rangle$ at $g = 0$, as given in (2). This method is not feasible for larger graphs, as discussed above on the quantum algorithm for HC problems.

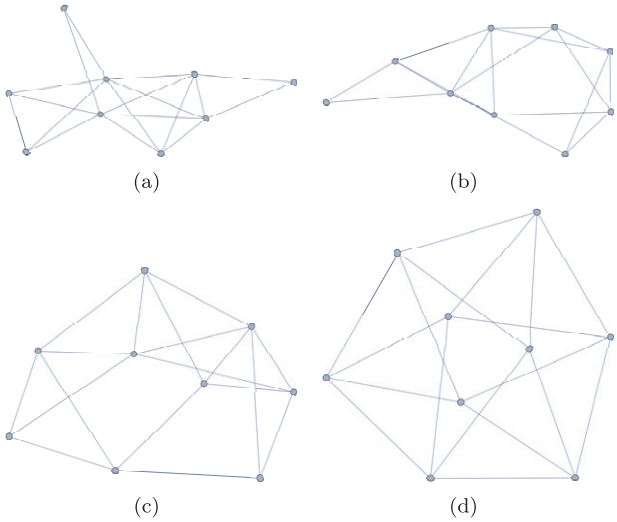

Fig. 3: Four different graphs, all with $N_v = 9$ and $N_e = 18$, corresponding to the 3×3 toroid lattice used in calculating the critical parameters of the TQPT of QZ2LGT. (a) G_1, with $N_{hc} = 0$. (b) G_2, with $N_{hc} = 10$. (c) G_3, with $N_{hc} = 30$. (d) G_4, with $N_{hc} = 48$.

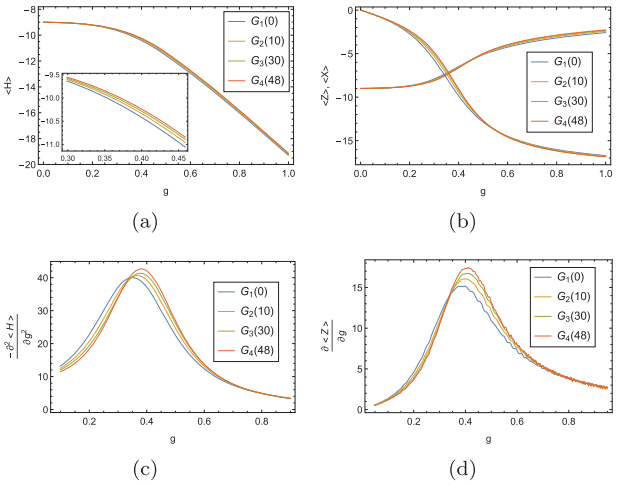

Fig. 4: Physical properties calculated for four graphs $G_i(N_{hc})$, $i = 1,2,3,4$. (a) $\langle H\rangle$. (b) $\langle Z\rangle$ and $\langle X\rangle$, which increase and decreases with g, respectively. (c) The second derivatives of $\langle H\rangle$ with respect to g. (d) The first derivative of $\langle Z\rangle$ with respect to g.

Then we adiabatically increase g from 0 to 1, in steps with $g_s = 0.001, t_s = 0.1, n = 100$, where g_s is the variation of g, t_s and n are the time and the number of the symmetric Trotter substeps within each step, respectively [7]. The total cumulative error is $\varepsilon_{all} = \sum_{g=g_s}^{1}\varepsilon_s(t,n,g)$, which is less than 0.135% for the graphs studied here.

We study QPTs on the lattices dual to these graphs. First, $\langle H\rangle$, $\langle Z\rangle$ and $\langle X\rangle$ are obtained as functions of g. Then we define two critical parameters, as estimations of the critical parameter g_c. One is the extremal point g_c^H of the second derivative of $\langle H\rangle$, the other is the extremal point g_c^Z of the first derivative of $\langle Z\rangle$. $\lambda_c^H = \frac{1}{g_c^H}$, $\lambda_c^Z = \frac{1}{g_c^Z}$.

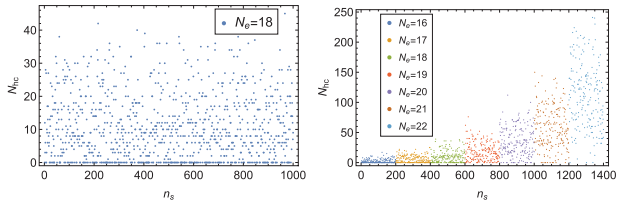

(a) (b)

Fig. 5: Distribution of N_{hc} in a random set of graph samples. n_s represents the number of the graphs. (a) $N_e = 18$ in each sample. There are 1000 samples in total. (b) N_e varies from 16 to 22. There are 200 samples with each value of N_e, and 1400 samples in total.

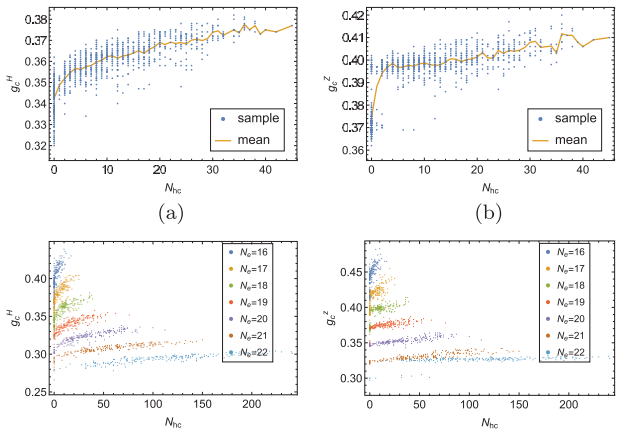

(a) (b)

(c) (d)

Fig. 6: Dependence of the critical parameters on N_{hc}. (a) Dependence of g_c^H on N_{hc} in graphs with $N_e = 18$. (b) Dependence of g_c^Z on N_{hc} in graphs with $N_e = 18$. (c) Dependence of g_c^H on N_{hc} in graphs with N_e varying from 16 to 22. (d) Dependence of g_c^Z on N_{hc} in graphs with N_e varying from 16 to 22.

As can be observed in fig. 4, g_c^H and g_c^Z both increase with N_{hc}. This verifies that the properties of the graph directly affect the characteristics of QPT.

In order to study how g_c^H and g_c^Z depend on N_{hc}, we prepare two groups of undirected and unweighted connected graphs with $N_v = 9$. The first group consists of 1000 samples, each with $N_e = 18$. We ran the classical GPU demonstration of the adiabatic quantum simulation, and obtained N_{hc} for each graph. The distribution of N_{hc} is shown in fig. 5(a). The second group consists of 200 graphs for each value of N_e varying from 16 to 22. The distribution of N_{hc} is shown in fig. 5(b).

It can be seen from fig. 6 that for given N_e, the average values of g_c^H and g_c^Z increase steadily with N_{hc}. Especially, when $N_{hc} = 0$, g_c^H and g_c^Z are very small. This implies that N_{hc} has a significant effect on g_c, which helps determine N_{hc} without actually searching the HCs of the graph. The time complexity required to reach TQPT is O_1.

Furthermore, we find that the relation between the average values of g_c^H and N_{hc} can be very well fitted as

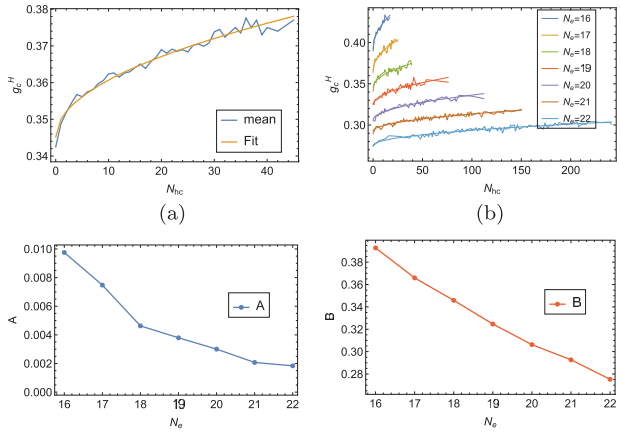

(a) (b)

(c) (d)

Fig. 7: Average value of g_c^H as a function of N_{hc}, fitted with $g_c^H = A\sqrt{N_{hc}} + B$. (a) Samples with $N_e = 18$. $A = 0.0049005$, $B = 0.345178$. (b) Sample with N_e varying from 16 to 22, with A and B depending on N_e. (c) Dependence of A in (b) on N_e. (d) Dependence of B in (b) on N_e.

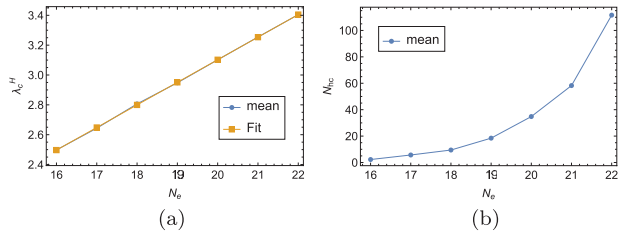

(a) (b)

Fig. 8: (a) λ_c^H as a function of N_e, fitted with $\lambda_c^H = 0.1513 * N_e + 0.07536$. N_e varies from 16 to 22. (b) Dependence of the average value of N_{hc} on N_e, which varies from 16 to 22.

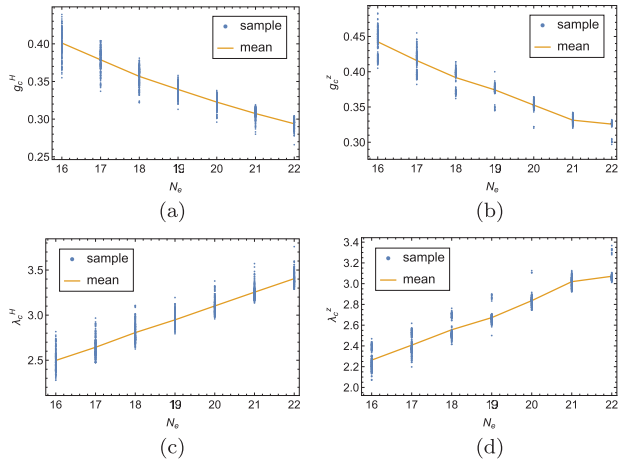

(a) (b)

(c) (d)

Fig. 9: Dependence of the critical parameters on N_e in samples with N_e varying from 16 to 22. (a) g_c^H. (b) g_c^Z. (c) λ_c^H. (d) λ_c^Z.

$g_c^H = A\sqrt{N_{hc}} + B$, as shown in fig. 7 for the two groups of graph samples, and the relation between λ_c^H and N_e can be very well fitted as $\lambda_c^H = 0.1513 * N_e + 0.007536$, as shown in fig. 8. These two relations are consistent. However, it

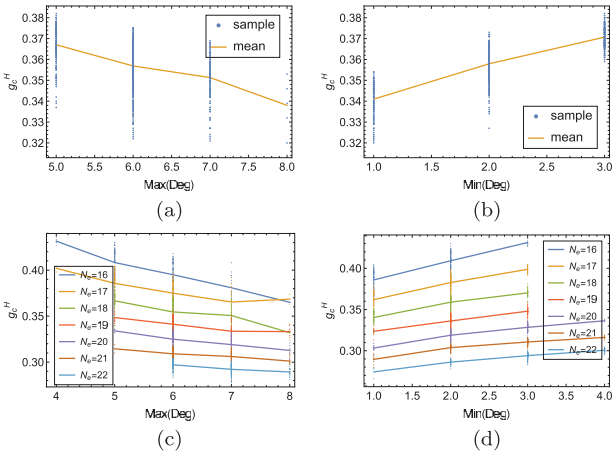

Fig. 10: Dependence of the critical parameters on the degrees of vertices. (a) Dependence of g_c^H on Max(Deg) in samples with $N_e = 18$. (b) Dependence of g_c^H on Min(Deg) in samples with $N_e = 18$. (c) Dependence of g_c^H on Max(Deg) in samples with N_e varying from 16 to 22. (d) Dependence of g_c^Z on Min(Deg) in samples with N_e varying from 16 to 22.

should be noted that due to the limitation of computing power, N_e is still relatively small in our simulated graphs, moreover, the relations in larger graphs are not yet known.

We have also studied the effect of N_e on the critical parameters, by using the second group of graphs with the same N_v but different N_e. As can be seen in fig. 9, the average values of g_c^H and g_c^Z decrease steadily with N_e for given N_v. The larger the N_e value, the smaller the critical parameters. In other words, the average value of $\lambda_c = \frac{1}{g_c}$ increases linearly with N_e for given N_v.

As shown in fig. 10, for given values of N_e and N_v, the average values of the critical parameters decrease with the maximal degree of the vertices Max(Deg), and increases with the minimal degree of the vertices Min(Deg). On average, when N_v and N_e are fixed, the larger Max(Deg), the smaller Min(Deg). So the dependence on Max(Deg) and the dependence on Min(Deg) are, as given in fig. 10, consistent.

Summary. – To summarize, we have developed a novel approach to the HC problem, by defining QZ2LGT on the lattice dual to the original graph. Moreover, we present a quantum adiabatic algorithm to obtain the closed-string condensate emerging at the TQPT, and find that the HC number N_{hc} of the graph has a significant effect on the TQPT critical parameter.

Given the importance of graph theory, our approach may also be useful for, say, deep learning, represented as deep neural networks and being integrated with graphical models [21,22], as well as quantum deep learning [23,24]. This work also suggests a new direction of research connecting graph problems with topological quantum matter.

* * *

This work was supported by National Natural Science Foundation of China (Grant No. 12075059).

Data availability statement: The data generated and/or analysed during the current study are not publicly available for legal/ethical reasons but are available from the corresponding author on reasonable request.

REFERENCES

[1] van Leeuwen J. (Editor), *Handbook of Theoretical Computer Science*, Vol. **B**: *Formal Models and Semantics* (MIT Press, Cambridge, Mass., USA) 1991.
[2] Garey M. R. and Johnson D. S., *Computers and Intractability; A Guide to the Theory of NP-Completeness* (W. H. Freeman & Co., USA) 1990.
[3] Kogut J. B., *Rev. Mod. Phys.*, **51** (1979) 659.
[4] Sachdev S., *Rep. Prog. Phys.*, **82** (2018) 014001.
[5] Lloyd S., *Science*, **273** (1996) 1073.
[6] Zohar E., Farace A., Reznik B. and Cirac J. I., *Phys. Rev. Lett.*, **118** (2017) 5.
[7] Cui X., Shi Y. and Yang J. C., *J. High Energy Phys.*, **2020** (2020) 160.
[8] Lamm H., Lawrence S. and Yamauchi Y., *Phys. Rev. D*, **100** (2019) 034518.
[9] Gnatenko Kh. P. and Susulovska N. A., *EPL*, **136** (2022) 40003.
[10] Huang Jieshan, Chen Xiaojiong, Li Xudong and Wang Jianwei, *AAPPS Bull.*, **33** (2023) 14.
[11] Lu Bo, Liu Lu, Song Jun-Yang, Wen Kai and Wang Chuan, *AAPPS Bull.*, **33** (2023) 7.
[12] Levin M. A. and Wen X. G., *Phys. Rev. B*, **71** (2005) 045110.
[13] Wen X. G., *Ann. Phys.*, **316** (2005) 1.
[14] Wegner F. J., *J. Math. Phys.*, **12** (1971) 2259.
[15] Freedman M., *Commun. Math. Phys.*, **234** (2003) 129183.
[16] Fradkin E., *Field Theories of Condensed Matter Physics* (Cambridge University Press, Cambridge) 2013.
[17] Hamma A. and Lidar D. A., *Phys. Rev. Lett.*, **100** (2008) 4.
[18] Trotter H. F., *Proc. Am. Math. Soc.*, **10** (1959) 545.
[19] Childs A. M., Su Y., Tran M. C., Wiebe N. and Zhu S., *Phys. Rev. X*, **11** (2021) 011020.
[20] Jones T., Brown A., Bush I. and Benjamin S. C., *Sci. Rep.*, **9** (2019) 10736.
[21] Johnson M. J., Duvenaud D., Wiltschko A. B., Datta S. R. and Adams R. P., *Composing graphical models with neural networks for structured representations and fast inference*, *NIPS'16: Proceedings of the 30th International Conference on Neural Information Processing Systems*, *Decemeber 2016*, pp. 2954–2962, arXiv:1603.06277 (March 2016).
[22] Wang H. and Yeung D., *IEEE Trans. Knowl. Data Eng.*, **28** (2016) 3395.
[23] Amin M. H., Andriyash E., Rolfe J., Kulchytskyy B. and Melko R., *Phys. Rev. X*, **8** (2018) 021050.
[24] Biamonte J., Wittek P., Pancotti N., Rebentrost P., Wiebe N. and Lloyd S., *Nature*, **549** (2017) 195.